Journal of Power Sources 196 (2011) 1904–1908

Contents lists available at ScienceDirect

Journal of Power Sources

journal homepage: www.elsevier.com/locate/jpowsour

Short communication

Carbon-nanosphere-supported Pt nanoparticles for methanol and ethanol electro-oxidation in alkaline media

Xue Wang[a], Chenguo Hu[a,*], Yufeng Xiong[b], Hong Liu[c], Guojun Du[c], Xiaoshan He[a]

[a] Department of Applied Physics, Chongqing University, 174 Shapingba Street, Chongqing 400044, PR China
[b] National Center for Nanoscience and Technology, Beijing 100080, PR China
[c] State Key Laboratory of Crystal Materials, Shandong University, Jinan 250100, PR China

ARTICLE INFO

Article history:
Received 18 August 2010
Received in revised form 7 September 2010
Accepted 20 September 2010
Available online 1 October 2010

Keywords:
Chemical synthesis
Carbon nanospheres
Pt nanoparticles
Fuel cell

ABSTRACT

Carbon nanospheres with diameters ~200 nm have been synthesized from glucose at 200 °C and normal atmosphere by a novel composite-molten-salt (CMS) method. Pt nanoparticles supported on those carbon nanospheres are used for methanol and ethanol electro-oxidation in alkaline media. Experimental results demonstrate that, in comparison with the carbon black or hydrothermally-synthesized carbon nanosphere support, CMS carbon-nanosphere-supported Pt electrocatalyst shows an enhanced efficiency for both methanol and ethanol electro-oxidation in terms of electrode conductivity, electrochemically active surface, oxidation peak current density and onset potential. This enhancement is considered to be not only due to the high carbonization of the CMS synthesized carbon nanospheres, but also due to the formation of a porous structure by the carbon nanospheres which significantly reduces the liquid sealing effect allowing efficient gas diffusion.

1. Introduction

Fuel cells have been receiving greater attention recently due to concern for the possible depletion of fossil fuels and increases in environmental pollution. Among the different types of fuel cells, direct methanol and ethanol fuel cells may become excellent power sources due to their high energy density, low pollution, low operating temperature, and their ease of handling [1]. Pt-based catalysts are recognized as the best candidates for low temperature fuel cells. However, the high cost and scarce supply of Pt limit the use of the Pt-based electrocatalysts. Numerous studies have been devoted mainly to the development of novel catalysts, including binary Pt alloy catalysts (e.g., PtRh, PtRu, PtNi [2–4]), ternary alloy catalysts (e.g., $PtWO_{3x}$ [5,6]), and quaternary catalysts (e.g., PtRuSnW [7]). Also, it has been proven that if direct alcohol fuel cells (DAFCs) operate in an alkaline instead of an acidic electrolyte the reaction kinetics of both the alcohol anodic oxidation and the oxygen cathodic reduction will be significantly improved [8–10]. These electrolyte-dependent properties make it possible to reduce the use of noble metal catalysts or substitute them with non-noble metal catalysts.

In addition to catalyst preparation, the choice of a suitable catalyst support can enhance the catalytic activity and reduce the use of noble metal catalysts. Carbon-related nanomaterials are considered to be one of the most ideal catalyst supports for fuel cells and have been widely used. In the past decades, carbon black has been most frequently used as a catalyst support [11–14], especially for Pt or Pt alloy electrodes for the oxygen cathode, or low-loading Pt electrodes for a hydrogen anode in an acid fuel cell. Recently, the appearance of novel carbon materials, such as graphite nanofibers (GNFs) [15], carbon nanotubes (CNTs) [16], coin-like carbon materials [17], fullerenes [18], carbon micro-trees [19], and carbon nanorods [20], has provided new candidates for carbon supports. In the previous reports, carbon spheres prepared by different methods have been proven as promising catalyst supports for fuel cells. Xu et al. [21] and Yang et al. [22] used carbon spheres obtained by the hydrothermal synthesis as supports for Pt and Pd catalysts for methanol and ethanol electrooxidation. Chai et al. [23] exploited spherical carbon capsules synthesized by using removable colloidal silica crystalline templates by carbonization of phenol and formaldehyde as a highly efficient catalyst support in direct methanol fuel cell.

In this paper, we develop a composite-molten-salt (CMS) method to synthesize carbon nanospheres in melts at lower temperature and ambient pressure. Though bulk materials have long been prepared by using the molten-salt synthesis method at high temperature, the preparation of uniform, small-sized materials using this technique at lower temperature has been only recently developed, and a limited number of nanomaterials have been reported [24–26]. This is the first time that carbon-related nano-

* Corresponding author. Tel.: +86 23 65104741; fax: +86 23 65105925.
E-mail addresses: hucg@cqu.edu.cn, hu.chenguo@yahoo.com (C. Hu).

0378-7753/$ – see front matter © 2010 Elsevier B.V. All rights reserved.
doi:10.1016/j.jpowsour.2010.09.072

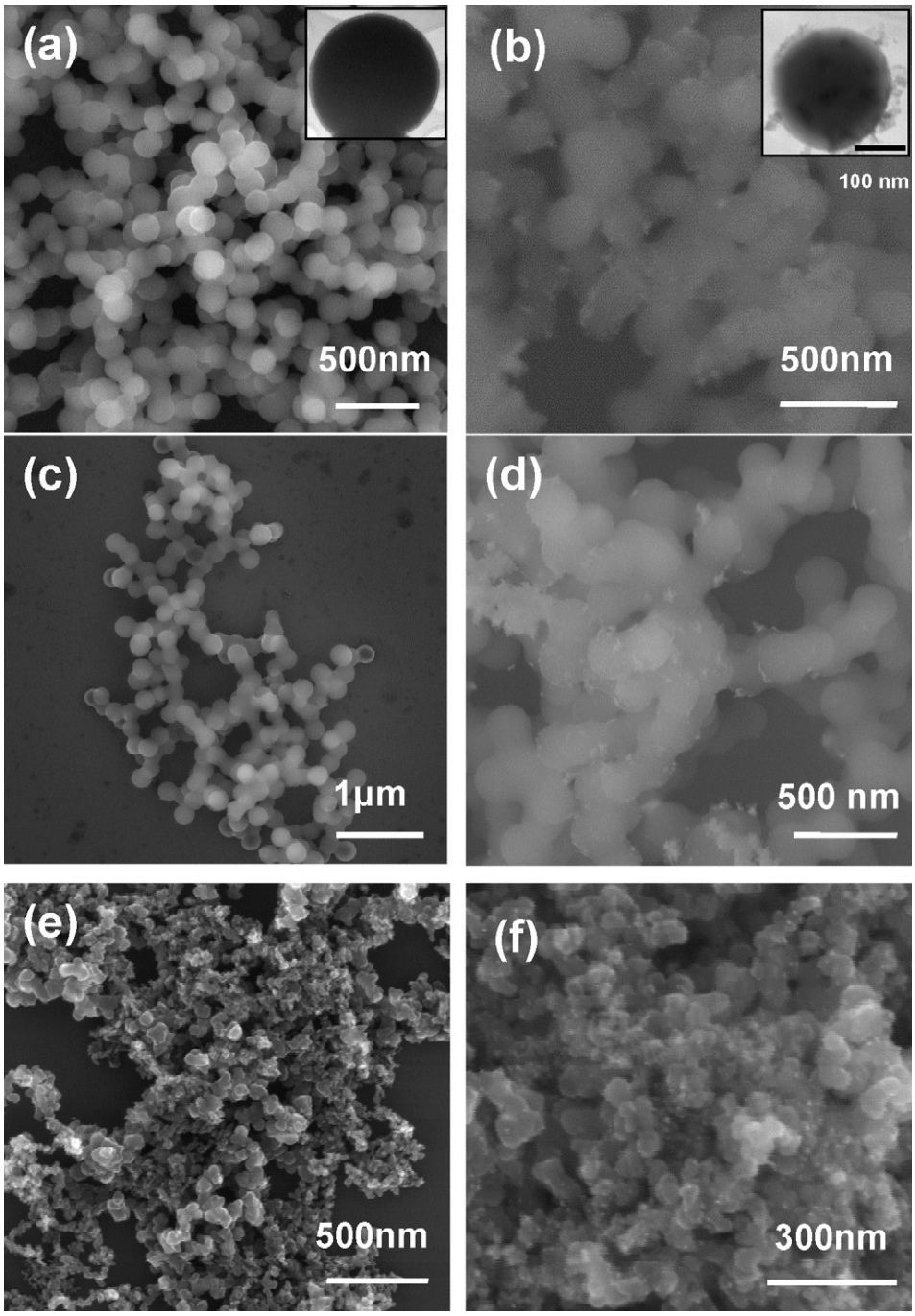

Fig. 1. FESEM image of carbon nanospheres synthesized by the CMS method. TEM image in inset (a). FESEM image of Pt nanoparticles supported on CMS carbon nanospheres. TEM image in inset (b). FESEM image of carbon nanospheres synthesized by the hydrothermal method (c) and Pt nanoparticles supported on them (d). FESEM image of carbon black (e) and Pt nanoparticles supported on carbon black (f).

material has been synthesized by the CMS method. The carbon nanospheres are obtained by dehydration and carbonization from pure glucose in a mixture of molten $KNO_3/LiNO_3$ salts at 200 °C and normal atmosphere without using any organic solvents or surfactants, which are commonly used for the preparation of polymer micro- or nanospheres. The as-prepared carbon nanospheres are used as a Pt catalyst support for direct methanol and ethanol electro-oxidation in alkaline media. Interestingly, the CMS carbon nanospheres thus prepared result in significantly increased catalytic activity in the fuel cell as compared with carbon nanospheres synthesized by the hydrothermal method and with commercially available carbon black.

2. Experimental

2.1. Reagents

Glucose, KNO_3, $LiNO_3$, KOH, $H_2PtCl_6{\cdot}6H_2O$, $NaBH_4$, isopropanol, HCl, Na_2SO_4, methanol and ethanol were purchased from Chongqing Chemical Reagent Company (Chongqing, China). Nafion and silver paste were purchased from Sigma–Aldrich and SPI Supplies. Carbon black (Vulcan XC72R) was from Cabot Corporation (Billerica, MA, USA). All chemicals were of analytical grade and were used as received. Deionized water was used throughout.

2.2. Synthesis of carbon nanospheres

In a typical experimental preparation, 9 g mixed KNO_3 and $LiNO_3$ with K/Li ratio of 58:42 was placed in a 25 mL Teflon vessel, then 0.5 g glucose was added in the vessel. The vessel was then placed in an oven preheated to 200 °C, which is higher than the normal glycosidation temperature and leads to aromatization and carbonization [27,28]. After this, the vessel was allowed to remain in the oven for 24 h for the reactions to fully take place. The vessel was then taken out and allowed to cool to room temperature naturally. The black product was collected by centrifugation and thoroughly washed with deionized water and ethanol.

Carbon nanospheres were also prepared from 0.5 g pure glucose, using the hydrothermal method at 200 °C for 24 h [29]. The product thus obtained was brown in color. The difference in color between the two synthesized carbon nanospheres indicated that the degree of carbonization of the CMS sample was higher than that prepared hydrothermally.

2.3. Preparation of carbon-supported Pt catalysts

Pt nanoparticles supported on carbon nanospheres obtained by the CMS, hydrothermal method, and carbon black were synthesized at room temperature by chemical reduction of $H_2PtCl_6{\cdot}6H_2O$ using $NaBH_4$. Briefly, a mixture of 0.005 g carbon nanomaterial, 0.0019 g $H_2PtCl_6{\cdot}6H_2O$, 0.1 mL HCl (0.37%) and 20 mL deionized water was put in a 50 mL beaker. Then 0.01 M $NaBH_4$ solution was added dropwise to the solution during continuous magnetic stirring until the color of the solution stabilized. Finally, the black product was washed with deionized water and ethanol several times.

2.4. Characterization

Raman spectrum (inVia Raman microscopes, Renishaw, UK) with an excitation line of 514.5 nm was utilized to identify the carbon nature of the sample synthesized by the CMS method. The size and morphology of the as-prepared products were measured by field emission scanning electron microscopy (FESEM, NOVA 400, FEI, Netherlands) and transmission electron microscopy (TEM, JEM-2100, JEOL, Japan). The crystal phase of the Pt particles was determined by X-ray diffractometer (XRD, BDX320, Peking University, China) with Cu Kα radiation (λ = 0.151418 nm).

2.5. Electrode fabrication and electrochemical measurements

Working electrodes were fabricated by casting the isopropanol-impregnated as-prepared Pt/carbon catalysts ink onto a graphite rod (G) electrode (radius, 0.6 cm), which was then allowed to dry at 60 °C under an infrared lamp. To immobilize the Pt/carbon nanostructures on the graphite electrode and to improve the anti-interference ability, 4 μL of 0.5 wt% Nafion was dropped on the surface of the electrode. The electrodes prepared by the CMS carbon, hydrothermal carbon and carbon black-supported Pt catalysts are labeled here Pt/MC/G, Pt/HC/G and Pt/BC/G electrodes, respectively. The Pt loading on each electrode was 0.65 mg cm^{-2}.

Electrochemical experiments were performed on LK98B(II) (Lanke, Tianjing, China) and CHI600C (CH Instrument, Shanghai Chenhua Instrument Corporation, China) electrochemical workstations. A standard three-electrode cell was used at room temperature (20 °C). A Pt foil and Ag/AgCl (saturated KCl) were used as the counter and reference electrode, respectively.

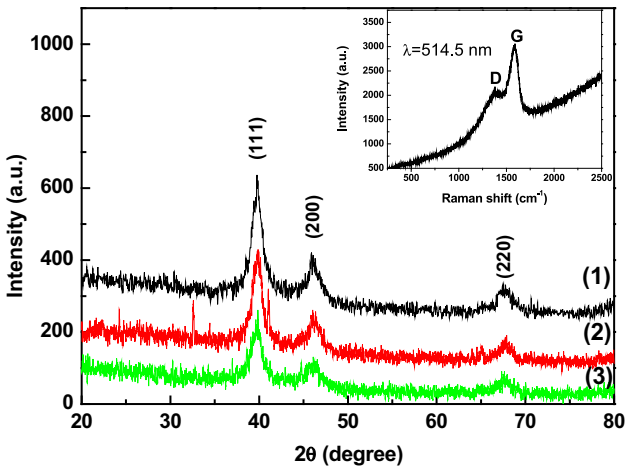

Fig. 2. XRD patterns of the as-prepared Pt/CMS carbon nanospheres (1), Pt/hydrothermal carbon nanospheres (2), Pt/carbon black (3). Raman spectra of carbon nanospheres synthesized by the CMS method in inset.

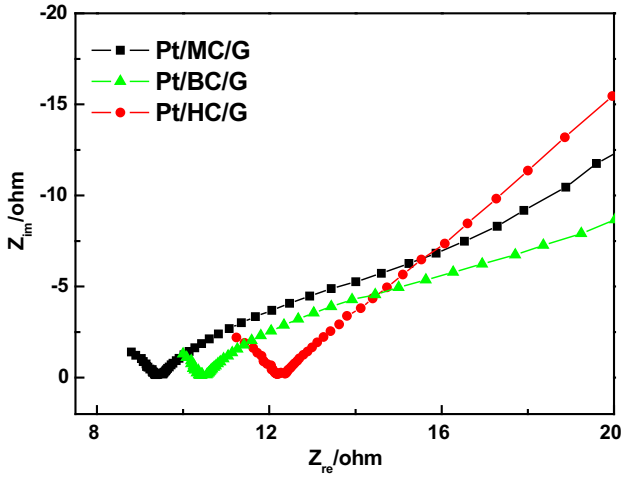

Fig. 3. EIS of the three different modified electrodes recorded from 1 to 100 kHz at the electrode potential +0.1 V (vs. Ag/AgCl) in 0.1 M Na_2SO_4 solution.

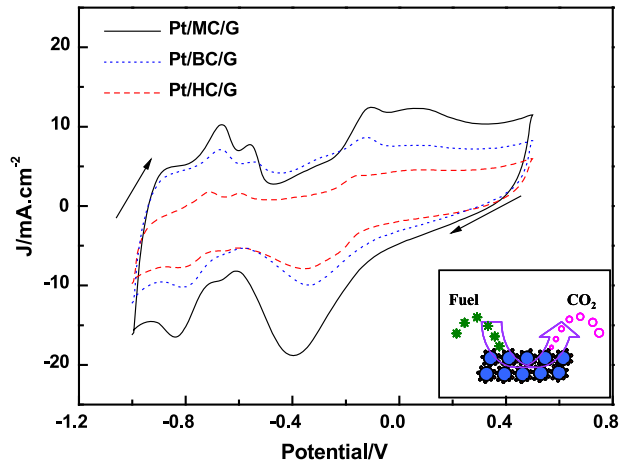

Fig. 4. CVs of the three different modified electrodes ran at 50 mV s^{-1} in 1.0 M KOH solution. Inset is a schematic diagram showing the porous structure of the carbon-nanosphere-supported Pt catalyst that significantly increases liquid channels and allows efficient gas diffusion.

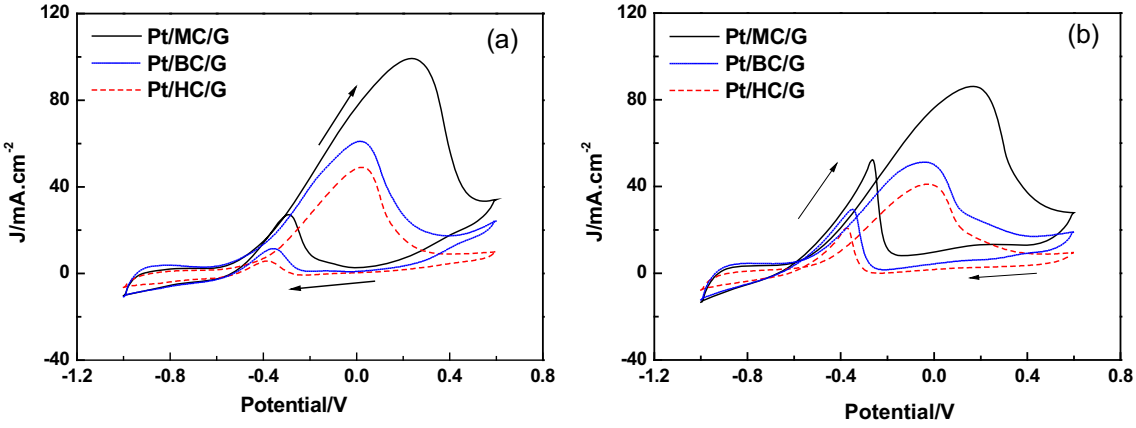

Fig. 5. CVs of the three different modified electrodes at 50 mV s^{-1} in 1.0 M KOH solution containing 1.0 M methanol (a) or 1.0 M ethanol (b).

3. Results and discussion

3.1. Structural characterization

Fig. 1 shows typical FESEM and TEM images of the as-synthesized carbon nanospheres and Pt/carbon catalysts. It can be observed from Fig. 1a that the sample synthesized by the CMS method consists of solid carbon nanospheres (TEM, as shown in inset) with diameter about 200 nm. After Pt catalyst deposition, the Pt nanoparticles appear homogeneously immobilized on the outer surface of the carbon nanospheres (Fig. 1b). Carbon nanospheres synthesized by the hydrothermal method (Fig. 1c) and Pt catalyst supported on them (Fig. 1d) have similar appearances to those obtained by the CMS method. The diameter of these spheres is about 250 nm. Fig. 1e shows the irregular morphology of the carbon black with much smaller dimensions varying from 20 to 100 nm. Pt nanoparticles are also deposited uniformly on the powder surface (Fig. 1f).

To confirm that the sample obtained by the CMS method is carbon, the sample was characterized by Raman spectroscopy, and the result is shown in the inset of Fig. 2. There are two strong bands centered at 1584 and 1378 cm^{-1}. The sharp peak at 1584 cm^{-1} (G-band) is attributed to the vibration of sp^2-bonded carbon atoms and indicates the fine graphitic structure of the CMS carbon nanospheres. The peak at 1378 cm^{-1} is assigned to the vibration of the D-band carbon atoms with dangling bonds in plane terminations of the disordered structure.

XRD patterns of the as-synthesized Pt/carbon composites are shown in Fig. 2. The peaks at $2\theta = 39.7^\circ$, 46.2° and 67.4° could be assigned to (1 1 1), (2 0 0) and (2 2 0) crystalline plane diffraction peaks, respectively, suggesting that the face-centered cubic platinum was successfully deposited on those carbon nanomaterials. The average size of the Pt nanoparticles is calculated based on the broadening of the (1 1 1) diffraction peak according to Scherrer's equation: $d = 0.9\lambda/B_{2\theta}\ \mathrm{Cos}\theta$, where λ represents the wavelength of the X-ray, θ is the angle of the peak, and $B_{2\theta}$ is the width of the peak at half height. The average size of Pt particles deposited on the three carbon nanomaterials are approximatley 8.45 nm.

3.2. Electrochemical performance of the fabricated electrodes

It is generally accepted that electrochemical impedance spectroscopy (EIS) is a useful method to characterize the electrochemical processes occurring at the solution/electrode interface. A typical electrochemical impedance spectrum presented in the form of a Nyquist plot (Z_{im} vs. Z_{re}) includes a semicircle region lying on the Z_{re}-axis at higher frequencies (related to the electron-transfer-limited process), followed by a linear part at lower frequencies (related to the diffusion-limited process). Usually, the semicircle diameter, which equals the electron-transfer resistance (R_{et}), is obviously affected by the surface modification of the electrode [30,31]. Fig. 3 shows the Nyquist plots of the three fabricated electrodes, recorded from 1 to 100 kHz at the electrode potential +0.1 V in 0.1 M Na_2SO_4 solution. As shown in Fig. 3, the values of R_{et} on the Pt/MC/G, Pt/BC/G and Pt/HC/G electrodes are 9.4, 10.4 and 12.2 Ω, respectively. This indicates that the conductivity of the Pt/MC/G electrode is higher than that of the other two electrodes. This higher

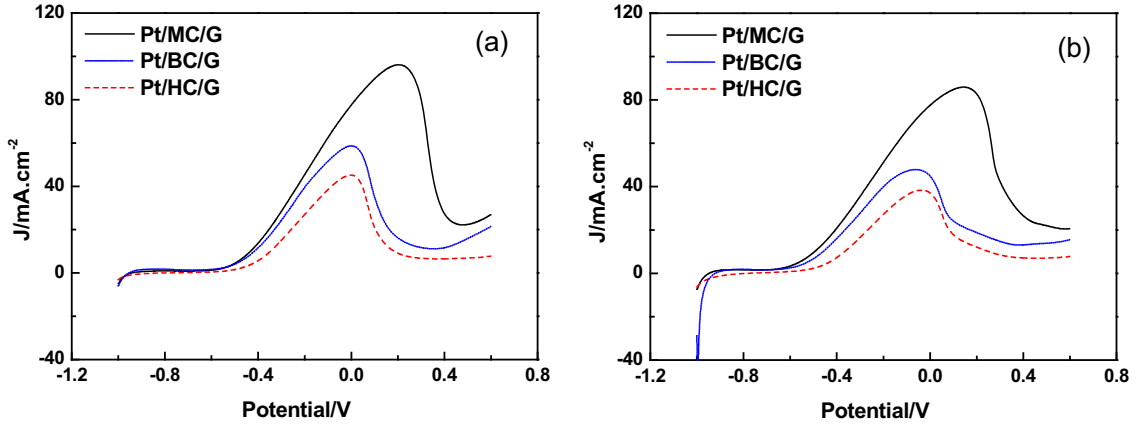

Fig. 6. Linear Sweep Voltammetry (LSV) of the three different modified electrodes at 50 mV s^{-1} in 1.0 M KOH solution containing 1.0 M methanol (a) or 1.0 M ethanol (b).

conductivity should improve the electrochemical oxidation process of ethanol and methanol.

Fig. 4 shows the typical cyclic voltammograms (CVs) of the three electrodes recorded in 1.0 M KOH solution from −1.0 to 0.5 V at a sweep rate of 50 mV s^{-1}. The similar peaks in the three curves in the potential region −0.8 to −0.5 V are associated with hydrogen adsorption process in the anodic scan [32,33]. According to the calculations of the CVs, the electrochemical active surfaces (EASs) of the three electrodes with the same Pt loading are in the order of Pt/MC/G > Pt/BC/G > Pt/HC/G. This result implies that the larger three-phase interface forms on Pt/MC/G electrode due to the porous structure formed by the carbon nanospheres. The carbon nanospheres act as structure units to form pores and channels that significantly reduce the liquid sealing effect [21,34,35]. These pores cause the liquid fuel to diffuse into the inside and the gaseous product (CO_2) to escape from the catalyst layer more easily (as shown in the inset of Fig. 4). These effective channels reduce the concentration polarization. Additionally, previous studies have proven that carbon black is an amorphous powder with a low degree of graphitization, which is prone to undergo electrochemical corrosion. As its wider size distribution and irregular morphology, carbon black forms a large percentage of micropores within its structure, which reduces the Pt utilization because the reactants are inaccessible to Pt particles anchored inside the micropores, and also increases the transfer resistance of reactants, intermediates, and products. On the other hand, although the Pt/HC/G electrode has a similar structure to that of the Pt/MC/G electrode (Fig. 1), the poor conductivity indicated by the EIS (Fig. 3) results in a consequent poor electrocatalyst performance.

Fig. 5 shows the typical CVs of methanol (a) and ethanol (b) electrooxidation on the three electrodes. The experiments were performed in 1.0 M KOH solution containing 1.0 M methanol or ethanol from −1.0 to 0.6 V at a sweep rate of 50 mV s^{-1}. Not surprisingly, peak current densities are larger on the Pt/MC/G electrode (99.6 mA cm^{-2} for methanol and 86.5 mA cm^{-2} for ethanol) than that on the Pt/BC/G electrode (61.6 mA cm^{-2} for methanol and 51.6 mA cm^{-2} for ethanol) and on the Pt/HC/G electrode (48.8 mA cm^{-2} for methanol and 41.5 mA cm^{-2} for ethanol) because of its good conductivity and high EASs.

To further study the onset potential for methanol and ethanol electrooxidation on the three electrodes, linear sweep voltammetry (LSV) in 1.0 M KOH solution containing 1.0 M methanol or ethanol was performed. The scan rate was 50 mV s^{-1} over a potential range from −1.0 to 0.6 V, and results are shown in Fig. 6. These results show that for both methanol (a) and ethanol (b) electrooxidation, the onset potential on Pt/MC/G electrode shows negative shift compared to that of the other two electrodes. This shift indicates improved reaction kinetics due to synergistic effect by the interaction between Pt and CMS carbon nanospheres. [21]

4. Conclusion

This study describes a new approach called composite-molten-salt (CMS) method for the synthesis of carbon nanospheres. Compared to the previous synthesis methods, the CMS method has the advantages of being simple, cost-effective, environmentally friendly and can be operated under normal atmospheric pressure and low temperature. The Pt catalyst supported on the CMS carbon nanospheres exhibits a much higher catalytic activity for methanol and ethanol electrooxidation in alkaline media than that of the Pt catalyst supported on the carbon black or on the hydrothermal synthetic carbon nanospheres. This higher catalytic activity is attributed to the high carbonization and good conductivity resulting from the new synthesis method. Additionally, the porous structure formed by the CMS carbon nanospheres reduces the liquid sealing effect and allows efficient gas diffusion.

Acknowledgments

This work is supported by the NSFC (60976055), Postgraduates' Science and Innovation Fund (201005B1A0010339) and Innovative Training Project (S-09109) of the 3rd-211 Project, and the large-scale equipment sharing fund of Chongqing University. The authors thank Dr. Bryan Baker in MSE at Georgia Tech for English language editing.

References

[1] L.F. Dong, R.R.S. Gari, Z. Li, M.M. Craig, S.F. Hou, Carbon 48 (2010) 781–787.
[2] V. Di Noto, E. Negro, J. Power Sources 195 (2010) 638–648.
[3] H.M. Saffarian, R. Srinivasan, D. Chu, S. Gilman, Electrochim. Acta 44 (1998) 1447–1454.
[4] S.Y. Shen, T.S. Zhao, J.B. Xu, Y.S. Li, J. Power Sources 195 (2010) 1001–1006.
[5] A.K. Shukla, M.K. Ravikumar, S. Arico, G. Candiano, V. Antonucci, N. Giordano, A. Hamnett, J. Appl. Electrochem. 25 (1995) 528–532.
[6] P.K. Shen, A.C.C. Tseung, J. Electrochem. Soc. 141 (1994) 3082–3090.
[7] A.S. Arico, Z. Poltarzewski, H. Kim, A. Morana, N. Giordano, V. Antonucci, J. Power Sources 55 (1995) 159–166.
[8] Y. Wang, L. Li, L. Hu, L. Zhuang, J.T. Lu, B.Q. Xu, Electrochem. Commun. 5 (2003) 662–666.
[9] J. Datta, S.S. Gupta, J. Power Sources 145 (2005) 124–132.
[10] D.J. Guo, H.L. Li, Carbon 43 (2005) 1259–1264.
[11] U.A. Paulus, U. Endruschat, G.J. Feldmeyer, T.J. Schmidt, H. Bonnemann, R.J. Behm, J. Catal. 195 (2000) 383–393.
[12] T. Frelink, W. Visscher, J.A.R. Van Veen, Electrochim. Acta 39 (1994) 1871–1875.
[13] K. Amine, K. Yasuda, H. Takenaka, Ann. Chim. Sci. Mater. 23 (1998) 331–335.
[14] O. Antoinea, Y. Bultel, R. Durand, J. Electroanal. Chem. 499 (2001) 85–94.
[15] J. Wang, R.P. Deo, P. Poulin, M. Mangey, J. Am. Chem. Soc. 125 (2003) 14706–14707.
[16] M.Y. Wang, J.H. Chen, Z. Fan, H. Tang, G.H. Deng, D.L. He, Carbon 42 (2004) 3257–3260.
[17] D.S. Yuan, C.W. Xu, Y.L. Liu, S.Z. Tan, X. Wang, Z.D. Wei, P.K. Shen, Electrochem. Commun. 9 (2007) 2473–2478.
[18] H.W. Kroto, J.R. Heath, S.C. O'Brien, R.F. Curl, R.E. Smalley, Nature 318 (1985) 162–163.
[19] P.M. Ajayan, J.M. Nugent, R.W. Siegel, B. Wei, P. Kohler-Redlich, Nature 404 (2000) 243.
[20] G.F. Zou, J. Lu, D.B. Wang, L.Q. Xu, Y.T. Qian, Inorg. Chem. 43 (2004) 5432–5435.
[21] C.W. Xu, L.Q. Cheng, P.K. Shen, Y.L. Liu, Electrochem. Commun. 9 (2007) 997–1001.
[22] R.Z. Yang, X.P. Qiu, H.R. Zhang, J.Q. Li, W.T. Zhu, Z.X. Wang, X.J. Huang, L.Q. Chen, Carbon 43 (2005) 11–16.
[23] G.S. Chai, S.B. Yoon, J.H. Kim, J.S. Yu, Chem. Commun. 23 (2004) 2766–2767.
[24] M. Wilbert, R. Rothe, K. Landfester, M. Antonietti, Chem. Mater. 13 (2001) 4681–4685.
[25] Y. Xi, C.G. Hu, X.M. Zhang, Y. Zhang, Z.L. Wang, Solid State Commun. 149 (2009) 1894–1896.
[26] C.H. Zheng, C.G. Hu, X.Y. Chen, H. Liu, Y.F. Xiong, J. Xu, B.Y. Wan, L.Y. Huang, Raspite PbWO4 nanobelts: synthesis and properties, Cryst. Eng. Comm. doi:10.1039/c004327c.
[27] G.C. Luijkx, F. van Rantwijk, H. van Bekkum, M.J. Antal Jr., Carbonhydr. Res. 272 (1995) 191–202.
[28] Q. Wang, H. Li, L.Q. Chen, X.J. Huang, Solid State Ionics 152 (2002) 43–50.
[29] Y.Z. Mi, W.B. Hu, Y.M. Dan, Y.L. Liu, Mater. Lett. 62 (2008) 1194–1196.
[30] H.L. Pang, J.P. Lu, J.H. Chen, C.T. Huang, B. Liu, X.H. Zhang, Electrochim. Acta 54 (2009) 2610–2615.
[31] X. Wang, C.G. Hu, H. Liu, G.J. Du, X.S. He, Y. Xi, Sens. Actuators B: Chem. 144 (2010) 220–225.
[32] C.G. Hu, X.S. He, C.H. Xia, J. Power Sources 195 (2010) 1594–1598.
[33] H.Y. Eileen, K. Scott, R.W. Reeve, J. Electroanal. Chem. 547 (2003) 17–24.
[34] Y.C. Liu, X.P. Qiu, Y.Q. Huang, W.T. Zhu, Carbon 40 (2002) 2375–2380.
[35] F.Y. Xie, Z.Q. Tian, H. Meng, P.K. Shen, J. Power Sources 141 (2005) 211–215.